

Supporting Information

Interface-assembled turn-on fluorescent nanofilm for highly selective detection of trifluoroacetic acid vapour via protonation-modulated ICT

Ling Zhang, Zebiao Qiu, Ruijuan Wen, Zhongrun Kang, Lingya Peng,* Rui Cao, Haonan Peng,*
and Yu Fang

Key Laboratory of Applied Surface and Colloid Chemistry (Ministry of Education), Shaanxi Key
Laboratory of New Conceptual Sensors and Molecular Materials, School of Chemistry and
Chemical Engineering, Shaanxi Normal University, Xi'an, Shaanxi 710119 (P. R. China)

*E-mail: phn@snnu.edu.cn; lingya.peng@snnu.edu.cn

Contents

1. Materials.....	3
2. Instrumental methods.....	3
3. Preparation of analyte vapors.....	3
4. Vapor sensing performance	4
5. Synthetic route of DTH-dimer-600.....	5
6. Synthetic route of DTH-DFP nanofilm	7
7. Basic optical properties	8
8. Macroscopic properties of DTH-DFP nanofilms.....	9
9. AFM image of DTH-DFP nanofilms	15
10. Structural characterization of DTH-DFP nanofilm.....	16
11. Sensing application of the DTH-DFP nanofilm for TFA.....	21
13. ¹ H NMR spectra	27
13. ¹³ C NMR spectra	30
14. HR-MS spectra	33

1. Materials

Polyethylene glycol (600, Adamas), *p*-toluoyl chloride (Adamas), dimethyl 2-hydroxyterephthalate (Bide Pharmatech Ltd.), 2-hydroxyisophthalaldehyde (Bide Pharmatech Ltd), hydrazine hydrate (80%, Shanxi Tongjie Chemical Reagent Co. Ltd), anhydrous dichloromethane (Adamas) and other routine chemicals used were obtained from commercial suppliers. Analytically pure solvents, including dichloromethane (DCM), anhydrous ether, acetone, dimethyl sulfoxide (DMSO), trichloromethane, tetrahydrofuran (THF), ethyl acetate (EAC), were purchased from National Pharmaceutical Reagent Co. (China). Detailed syntheses of the building blocks DTH-dimer-600-ester can be found in the Supporting Information.

2. Instrumental methods

The compounds were characterized by ¹H NMR (AV-600, AV-400, Bruker), functional groups on the surfaces of the film were verified by infrared spectrometer (FTIR, Bruker VERTEX70 V), and X-ray photoelectron spectrometer (XPS, AXIS ULTRA from Kratos Analytical Ltd). UV-Vis absorption spectra were recorded on a UV-Vis spectro-photometer (Hitachi U3900). Surface morphologies and thicknesses of the film were determined on field emission scanning electron microscope (SEM, SU8020, Hitachi) and atomic force microscopy (AFM, Dimension Icon atomic force microscope, Bruker). Contact angle was measured on a video-based contact angle measuring instrument (OCA20, Dataphysics). Fluorescence spectra were recorded on the fluorescence spectrometer with xenon lamp as the light source (FLS980, Edinburgh Instruments).

3. Preparation of analyte vapors

The procedure for generating analyte vapors is illustrated using trifluoroacetic acid (TFA) as an example. At ambient temperature, 10 mL of liquid TFA was introduced into a 500 mL brown

headspace vial. The vial was subsequently sealed and allowed to equilibrate at the designated test temperature for 12 hours to establish a saturated TFA vapor phase. Following equilibration, the headspace vapor was entirely withdrawn using a 500 mL gas-tight syringe and transferred into a dedicated gas-sampling bag. This resulting bag, designated as the standard vapor source, contained TFA at a concentration of 14,800 ppm. For the preparation of a 1,480 ppm TFA vapor sample, a separate clean syringe was used to extract a 50 mL aliquot of vapor from the standard source bag. This aliquot was then diluted with 450 mL of dry air. Samples at other desired concentrations were obtained accordingly by performing analogous serial dilution steps.

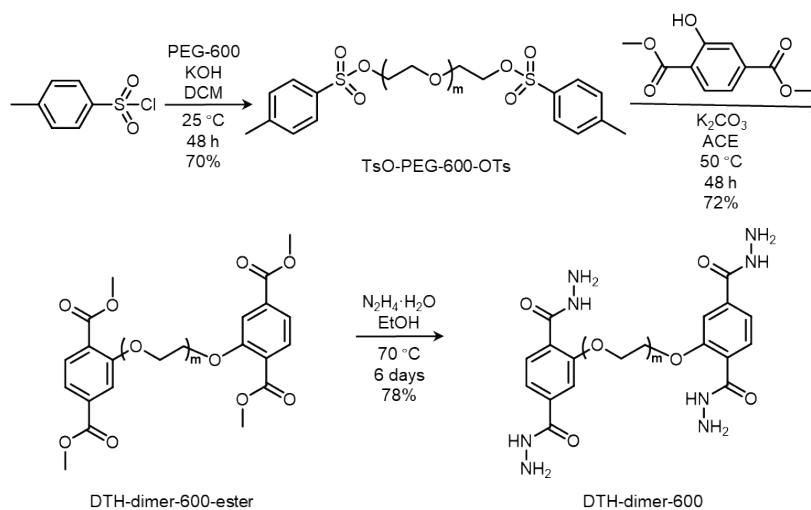
4. Vapor sensing performance

The nanofilm was integrated into a custom-built sensing device to evaluate its responsiveness to various analyte vapors. An auto sampling system with a controlled injection time of 2 s and at least 5 measurements of each vapor sample were used in the tests to ensure the accuracy of the experimental results. The nanofilm sensing performance was measured by the change in fluorescence intensity (I_0) of the film in dry air versus the fluorescence intensity (I) of the film after treatment with the analyzed vapors.

The saturated vapor concentration of the analyte (C_A) can be expressed by the following equation. Where the atmospheric pressure at the test temperature is P_{am} and the saturation vapor pressure of the analyte vapor at the test temperature is P_A . The analyte vapor is then mixed with dry air in a syringe to obtain the target concentration of vapor.

$$C_A = P_A / P_{am} \times 10^6$$

5. Synthetic route of DTH-dimer-600



Scheme S1. Synthetic route of DTH-dimer-600.

Synthetic route of TsO-PEG-600-OTs

PEG-600 (3 g, 5 mmol) was placed into a two-necked round-bottom flask under a nitrogen atmosphere. Subsequently, *p*-toluenesulfonyl chloride (2.39 g, 12.5 mmol), KOH (1.12 g, 20 mmol), and anhydrous dichloromethane (10 mL) as the solvent were added to the flask. The reaction mixture was stirred at room temperature for 48 h. Upon completion of the reaction, ultrapure water (25 mL) was added, and stirring was continued for an additional 30 minutes to quench the reaction. The resulting mixture was extracted three times with dichloromethane and 1 M hydrochloric acid aqueous solution. The combined organic layers were dried over anhydrous MgSO₄, filtered, and concentrated under reduced pressure using a rotary evaporator. The desired compound was obtained as a yellowish green viscous liquid (3.2 g) with a yield of 70% after drying.

¹H NMR (400 MHz, CDCl₃, 298 K) δ (ppm): 7.73 (d, J = 4 Hz, 4H), 7.28 (d, J = 8 Hz, 4H), 4.09 (dd, J = 9.0, 4.0 Hz, 4H), 3.63-3.50 (m, 48H), 2.37 (s, 6H).

¹³C NMR (600 MHz, CDCl₃, 298 K) δ (ppm): 144.81, 132.96, 129.83, 127.95, 68.63-70.50, 21.62.

HR-MS: [(M+H)]⁺ calculated for C₄₀H₆₇O₁₈S₂⁺: 899.3763; found m/z = 899.3773.

Synthetic route of DTH-dimmer-600-ester

TsO-PEG-600-OTs (950 mg, 1.04 mmol) was placed into a double-necked round-bottom flask under a nitrogen atmosphere. Subsequently, Diethyl 2,5-dihydroxyterephthalate (651 mg, 3.17 mmol), K₂CO₃ (575 mg, 4.16 mmol), and acetone (10 mL) as the solvent were added to the flask. The reaction mixture was heated at 60 °C for 48 h. The resulting mixture was extracted three times with dichloromethane and 1 M NaOH aqueous solution. The combined organic layers were dried over anhydrous MgSO₄, filtered, and concentrated under reduced pressure using a rotary evaporator. The desired compound was obtained as a yellow-brown viscous liquid (0.53 g) with a yield of 50% after drying.

¹H NMR (400 MHz, CDCl₃, 298 K) δ (ppm): 7.79 (d, J = 8 Hz, 2H), 7.64 (dd, J = 8.0 Hz, 3.0 Hz, 4H), 4.26 (dd, J = 4.0, 4.0 Hz, 4H), 3.95-3.88 (m, 16H), 3.78-3.60 (m, 44H).

¹³C NMR (600 MHz, CDCl₃, 298 K) δ (ppm): 166.11, 157.96, 134.30, 131.39, 124.76, 121.51, 114.35, 69.07-71.02, 52.48.

HR-MS: [(M+H)]⁺ calculated for C₄₀H₇₁O₂₂⁺: 975.4432; found m/z = 975.4436.

Synthetic route of DTH-dimer-600

DTH-dimer-600-ester (300 mg, 0.29 mmol) was placed into a double-necked round-bottom flask under a nitrogen atmosphere. Then, 2 mL of 80% hydrazine hydrate aqueous solution, and EtOH (10 mL) as the solvent were added to the flask. The reaction was stirred at 70 °C for six days. The reaction system was passed through a rotary evaporator to remove the solvent and hydrazine hydrate to get the brown colloidal solid product DTH-dimer-600 (0.22 mg) in 78% yield.

^1H NMR (400 MHz, DMSO- d_6 , 298 K) δ (ppm): 9.88 (s, 2H), 9.27 (s, 2H), 7.81 (d, $J = 16.0$ Hz, 2H), 7.55 (s, 2H), 7.50 (d, $J = 8.0$ Hz, 2H), 4.57 (s, 8H), 4.29 (dd, $J = 4.0, 4.0$ Hz, 4H), 3.81 (d, $J = 4.0$ Hz, 4H), 3.65-3.43 (m, 44H).

^{13}C NMR (600 MHz, DMSO- d_6 , 298 K) δ (ppm): 165.25, 164.24, 137.05, 130.93, 124.69, 120.09, 112.54, 68.81-70.35.

HR-MS: $[(\text{M}+\text{H})]^+$ calculated for $\text{C}_{42}\text{H}_{71}\text{N}_8\text{O}_{18}^+$: 975.4881; found $m/z = 975.4880$.

6. Synthetic route of DTH-DFP nanofilm

1.732 mg (1.79×10^{-3} mmol) of DTH-600-dimer and 0.268 mg (1.79×10^{-3} mmol) of DFP were placed into a 1.5 mL centrifuge tube, followed by the addition of 400 μL of DMSO. The mixture was subjected to 10 minutes of sonication, during which the fluorescence of the precursor solution transitioned from green to orange. A glass substrate (2 cm \times 2 cm) was meticulously cleaned via sequential ultrasonication in ethanol, dichloromethane, and again ethanol, followed by drying under ambient conditions. Subsequently, 100 μL of the precursor solution was drop-cast onto the prepared substrate. For scaled-up film fabrication, 5 mL of the same concentration precursor solution was uniformly applied to a 10 \times 10 cm glass plate. The coated substrate was then transferred to a controlled environment (25 $^\circ\text{C}$, 60% RH) for 12 hours. After this period, the glass plate was carefully immersed in a Petri dish containing ultrapure water, resulting in the formation of a uniform, transparent, and wrinkled nanofilm floating on the water surface. By modulating the preparation time, freestanding films with varying thicknesses could be obtained. Utilizing different substrate materials—such as glass plates, copper meshes, or silicon wafers—enabled the successful preparation of film samples suitable for subsequent investigation and characterization.

7. Basic optical properties

Their fluorescence quantum yields were measured by Quantum yield measurement system C9920-02G.

Table 1 Optical properties of DFP powder, TTPE-DTH-600-G film.

Sample	Excitation/ λ_{ma} x	Emission/ λ_{ma} x	$\Phi_F\%$
DFP powder	364 nm	533 nm	10.8
DTH-DFP nanofilm	370 nm	570 nm	3.4

8. Macroscopic properties of DTH-DFP nanofilms

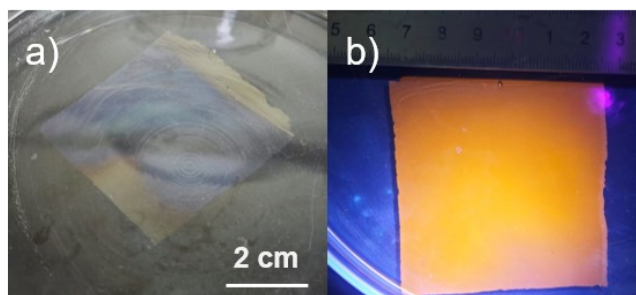


Figure S1. Preparation of DTH-DFP nanofilm with width of 6 cm. a) under day light, b) under UV light.



Figure S2. Processability DTH-DFP nanofilm.

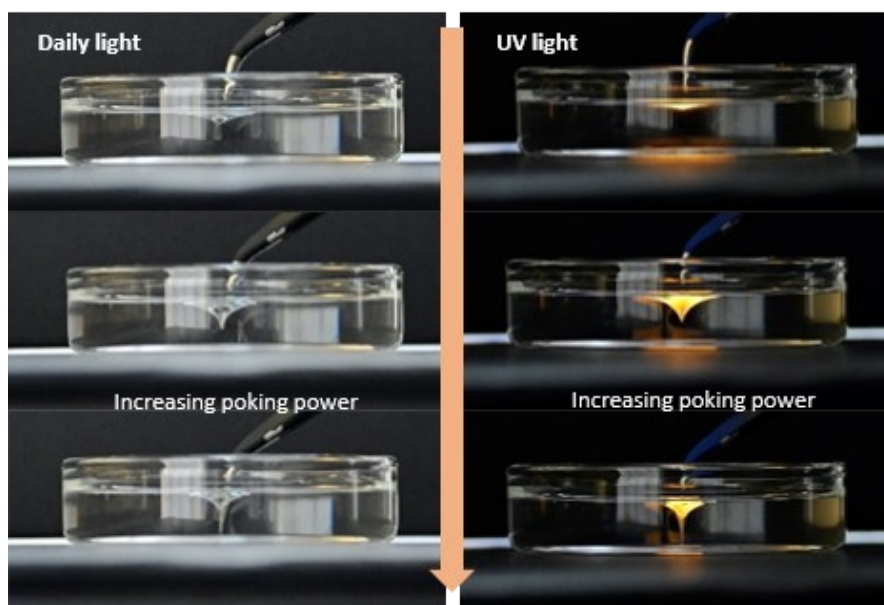


Figure S3. Mechanical Flexibility of DTH-DFP nanofilm.

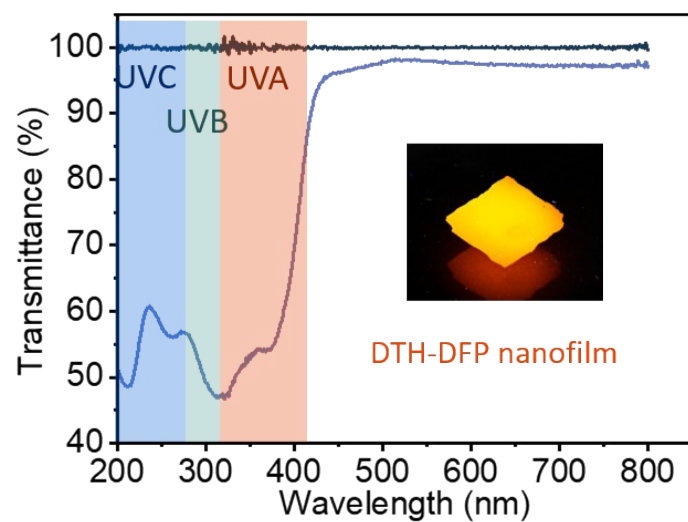


Figure S4. The UV-Vis absorption of the DTH-DFP nanofilm across the 200-800 nm spectral range.



Figure S5. Adhesion of DTH-DFP nanofilms on rubber surfaces, glass surfaces, and steel surfaces.

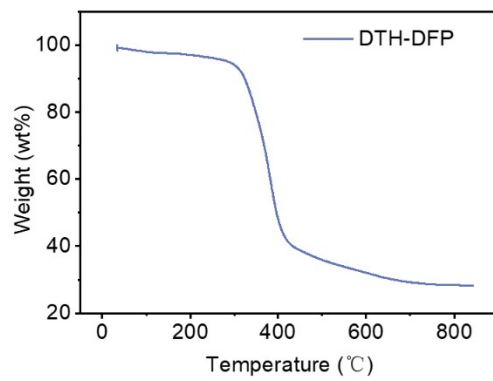


Figure S6. TGA curve of the DTH-DFP nanofilm.

9. AFM image of DTH-DFP nanofilms

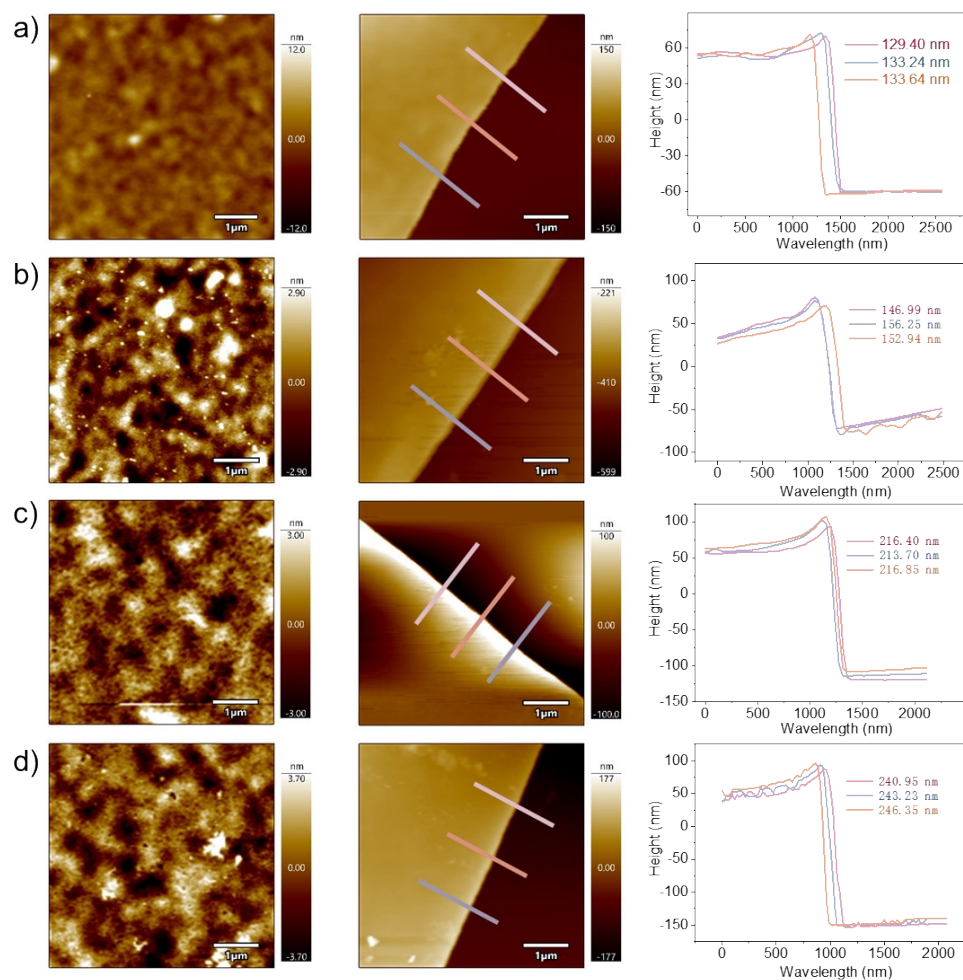


Figure S7. DTH-DFP nanofilms of different thicknesses obtained by controlling the preparation time. a) 12 h, b) 24 h, c) 36 h and d) 48 h.

10. Structural characterization of DTH-DFP nanofilm

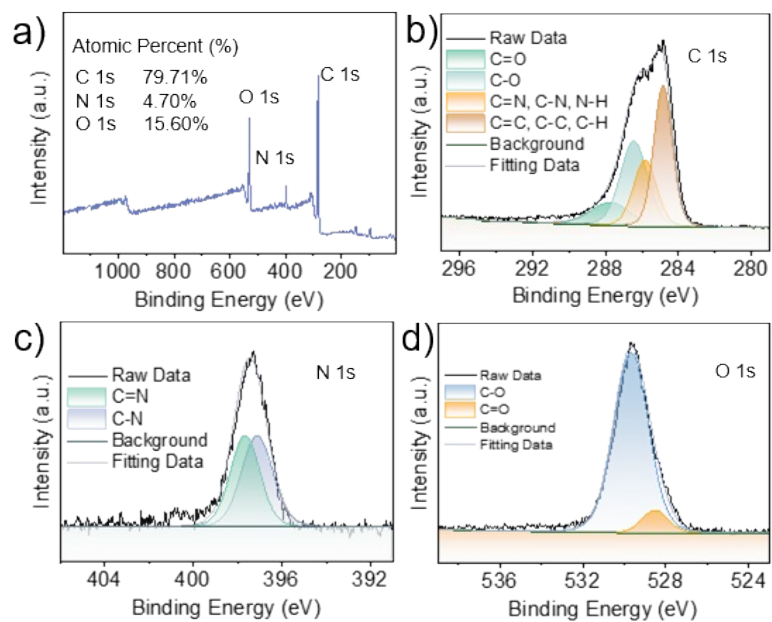


Figure S8. (a) XPS spectrum. (b) C 1s XPS spectrum (c) N 1s XPS spectrum. (d) O 1s XPS spectrum.

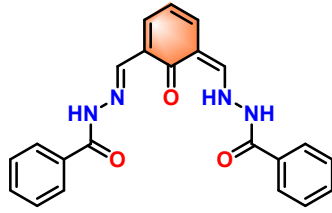


Figure S9. Simulation of the molecular structure in the DTH-DFP nanofilm.

Samples for XPS measurements were prepared by attaching DTH-DFP nanofilm samples to silicon wafers

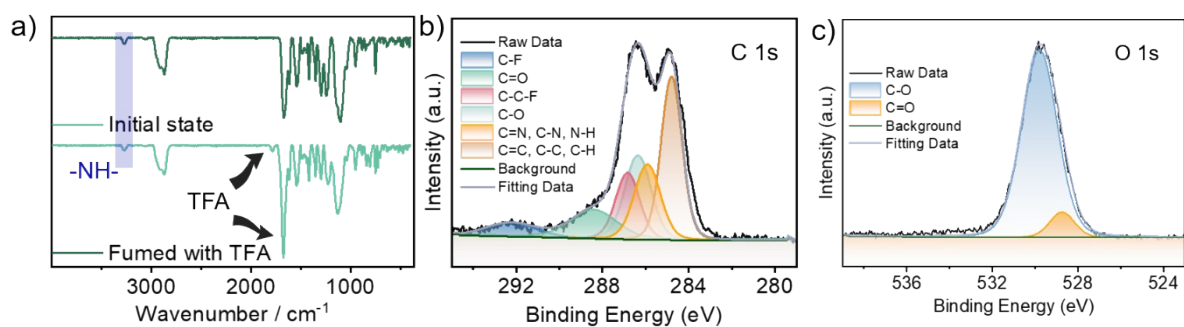


Figure S10. (a) FT-IR spectra before and after TFA treatment. (b) C 1s XPS spectrum after being treated with TFA. (c) O 1s XPS spectrum after being treated with TFA.

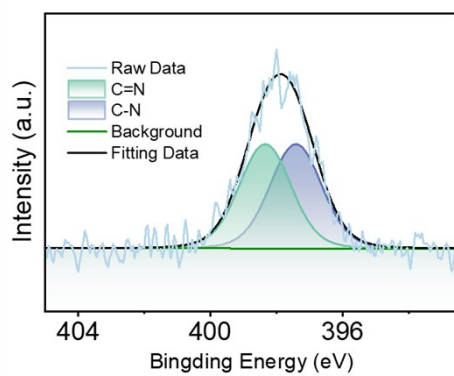


Figure S11. N 1s XPS spectrum after being treated with HCOOH vapour.

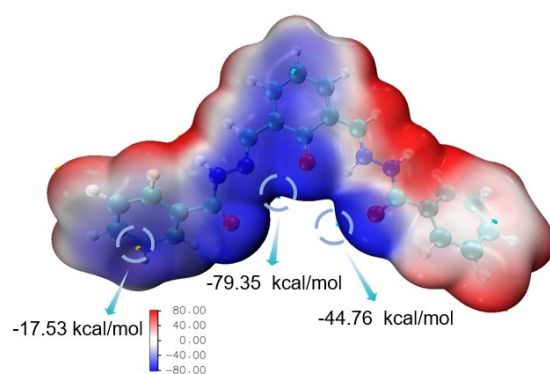


Figure S12. Theoretical surface electrostatic potential of the DTH-DFP nanofilm before protonation.

11. Sensing application of the DTH-DFP nanofilm for TFA

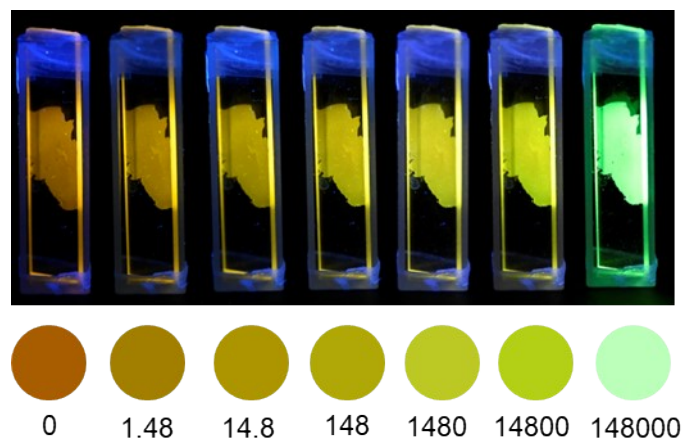


Figure S13. The fluorescence response of the DTH-DFP nanofilm to TFA vapor at various concentrations (ppm) under 365 nm UV light.

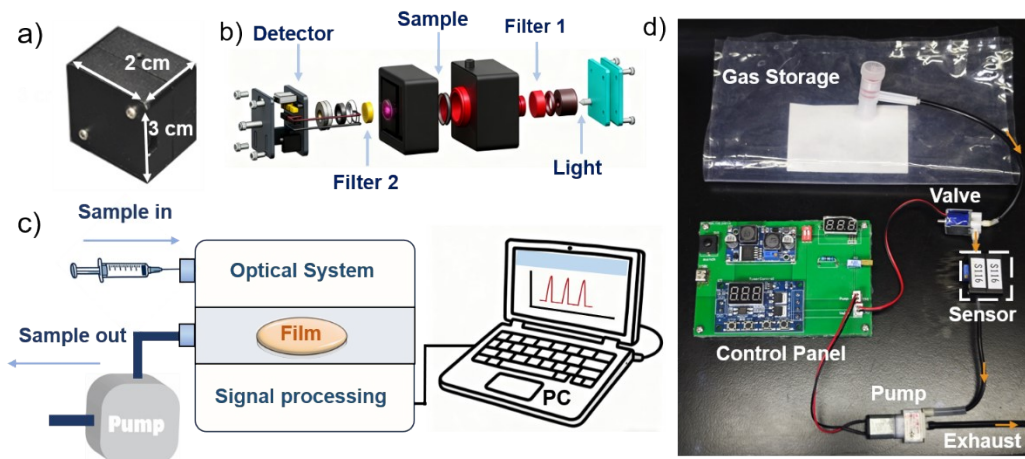


Figure S14. (a) Physical stacked optical sensor. (b) Schematic diagram of the hardware structure of a laminated optical sensor. (c) Schematic diagram of the self-built fluorescent sensing platform. (d) Schematic diagram of the real fluorescence sensing platform.

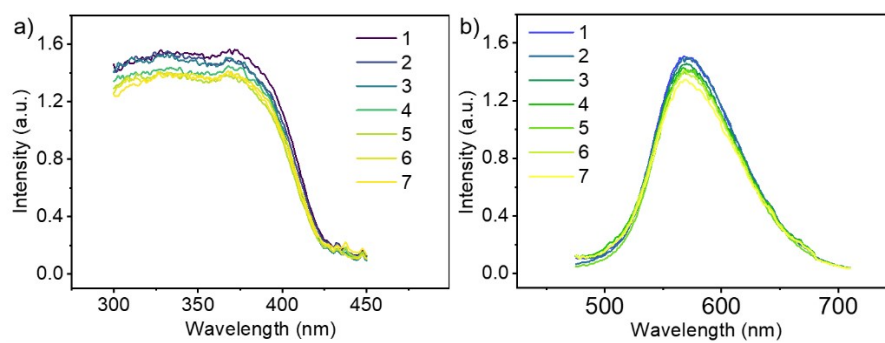


Figure S15. Spectral stability of the DTH-DFP nanofilm after 7-day exposure to indoor visible light and ambient air at room temperature. (a) Normalised excitation spectra ($\lambda_{em} = 570$ nm). (b) Normalised emission spectra ($\lambda_{em} = 365$ nm).

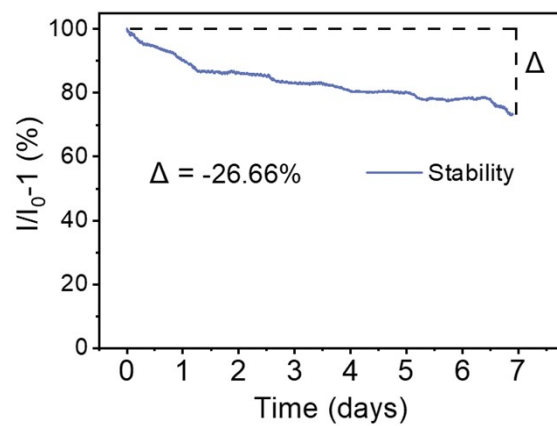


Figure S16. Photochemical stability of the DTH–DFP nanofilm under continuous 365 nm irradiation over 7 days.

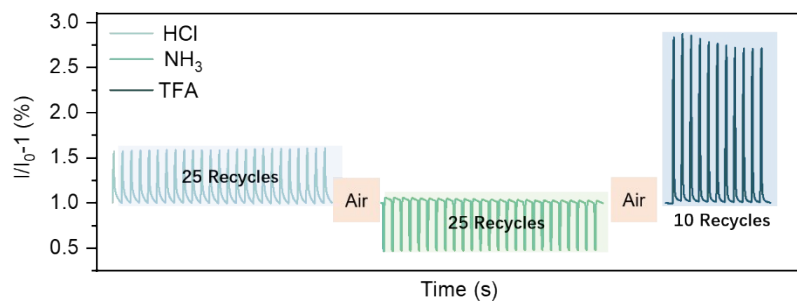


Figure S17. TFA sensing performance of the DTH–DFP nanofilm after chemical challenge tests. The film was pre-exposed to saturated HCl vapour (25 cycles) or saturated NH₃ vapour (25 cycles), followed by TFA sensing at 74,000 ppm under identical measurement conditions.

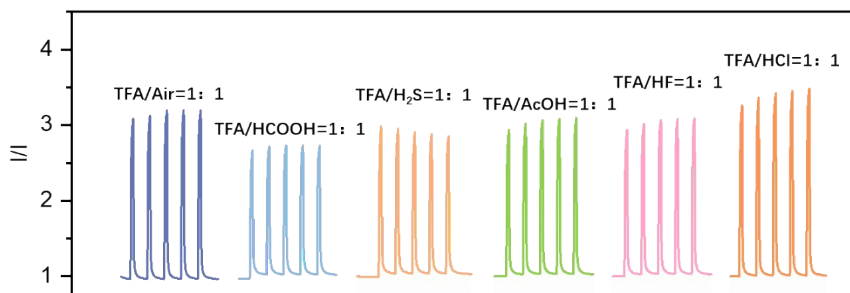


Figure S18. The sensor response upon exposure to a gas mixture (All VOCs are at saturated vapour concentration).

13. ^1H NMR spectra

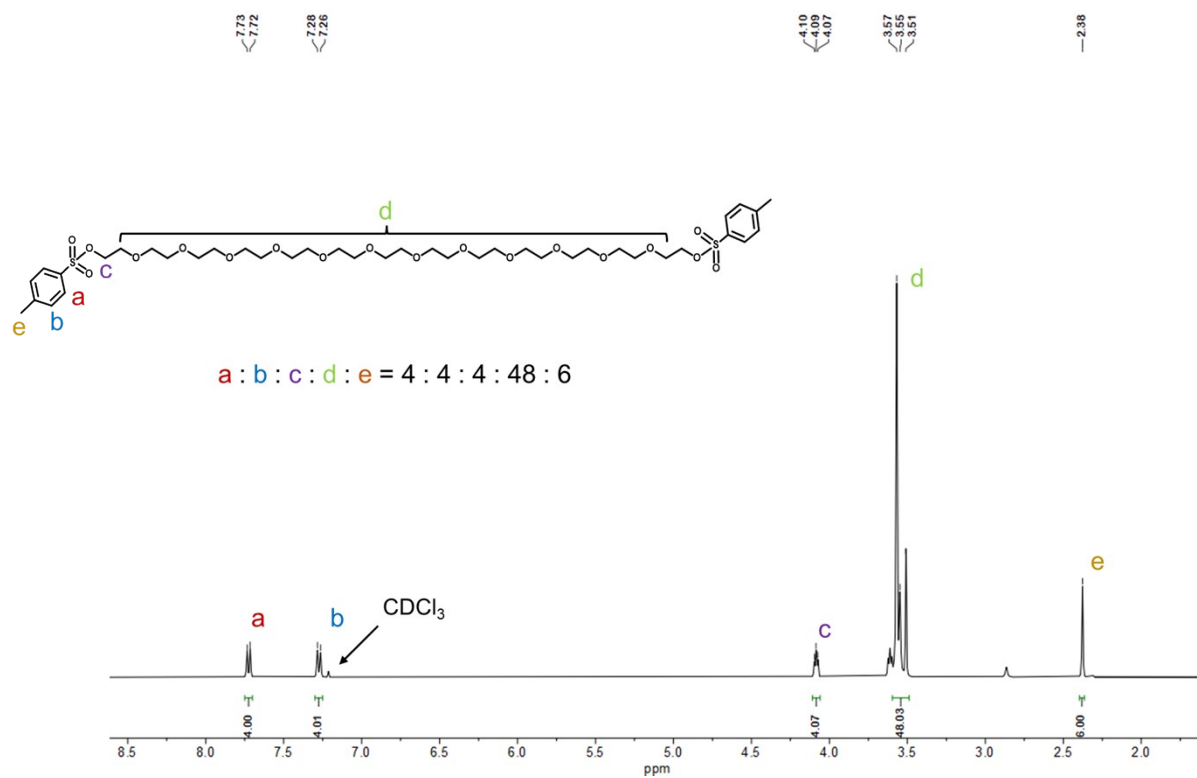


Figure S19. ^1H NMR spectrum of the compound TsO-PEG-600-OTs in CDCl_3 at 298 K.

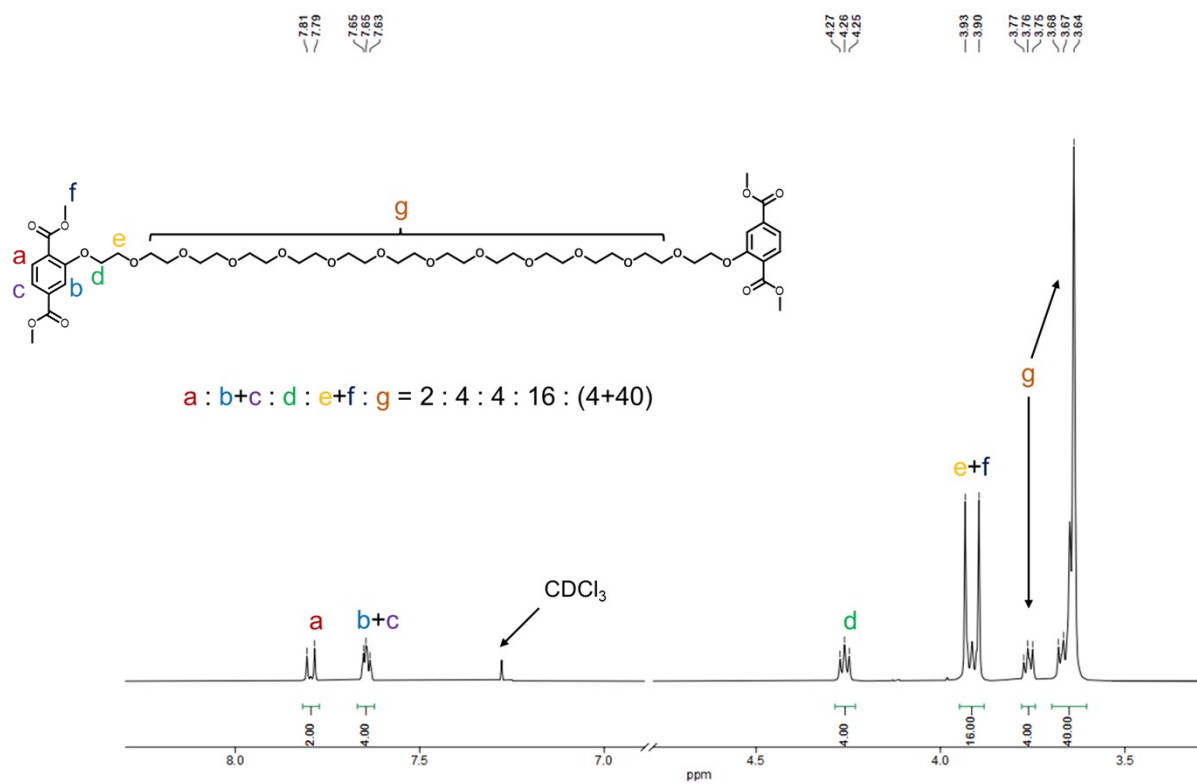


Figure S20. $^1\text{H NMR}$ spectrum of the DTH-dimer-600-ester in CDCl_3 at 298 K.

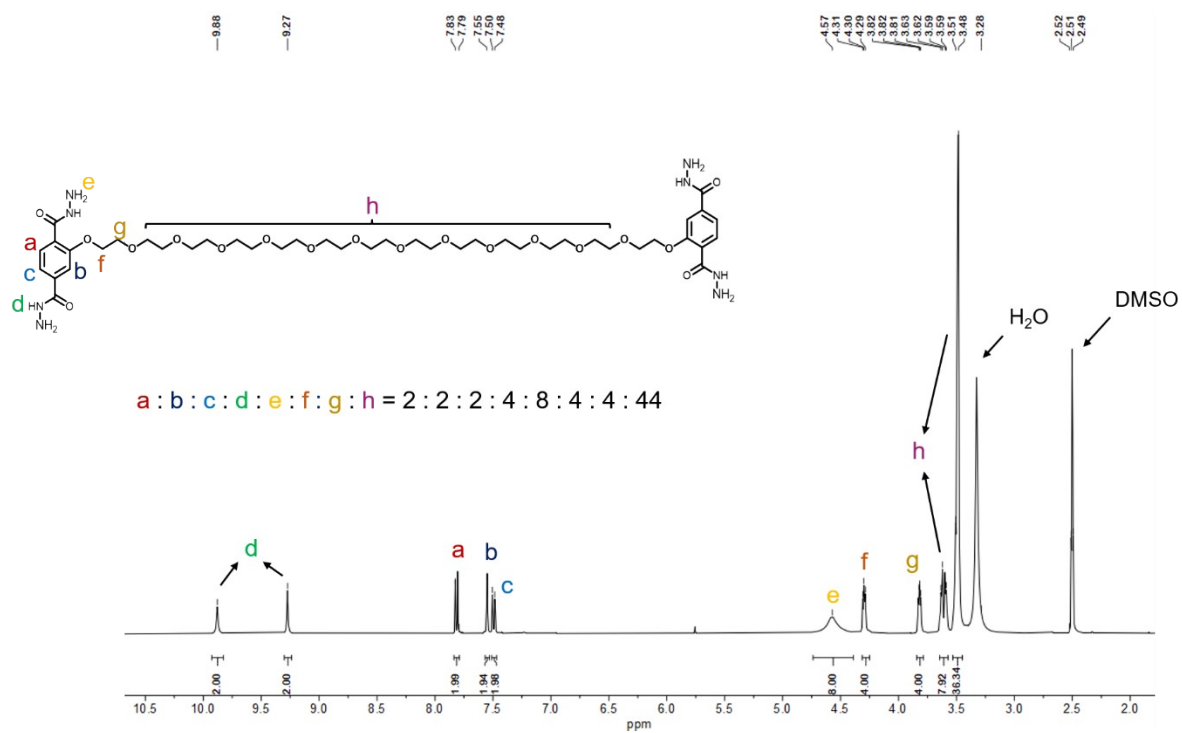


Figure S21. ¹H NMR spectrum of the DTH-dimer-600 in DMSO-d₆ at 298 K.

13. ¹³C NMR spectra

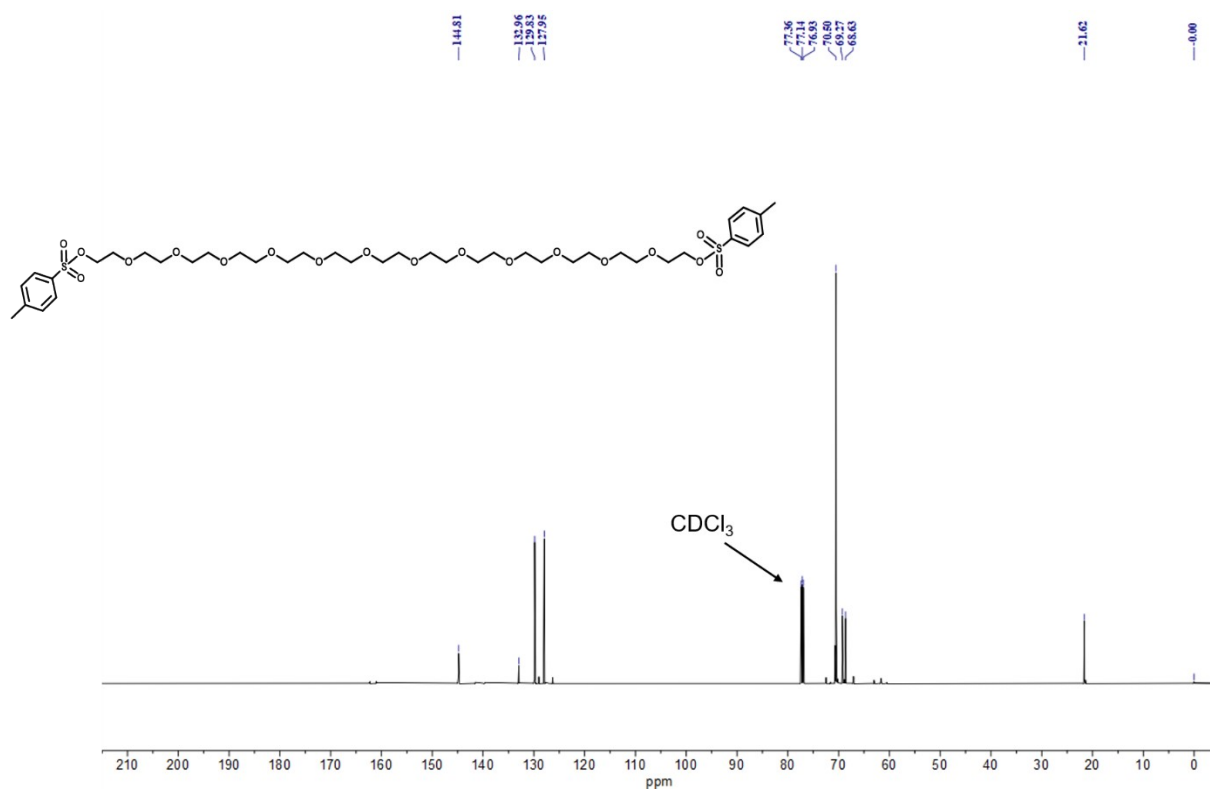


Figure S22. ¹³C NMR spectrum of the compound TsO-PEG-600-OTs in CDCl₃ at 298 K.

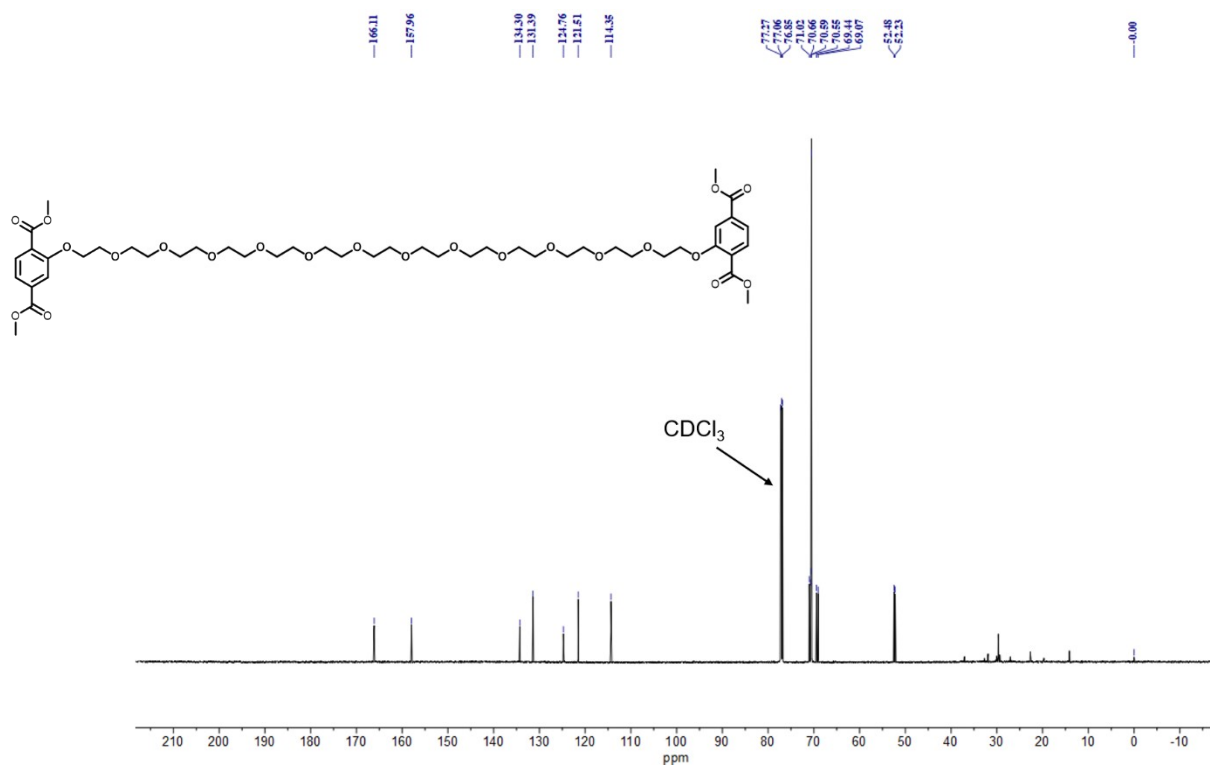


Figure S23. ¹³C NMR spectrum of the compound DTH-dimer-600-ester in CDCl₃ at 298 K.

14. HR-MS spectra

Although the PEG-600 reagents used in this work are oligomers with an average molecular weight of approximately 600, the peak at m/z 591 (indicated by the red dashed circles) was selected as the characteristic signal to monitor the reaction. The corresponding high-resolution mass spectrometry (HR-MS) spectra are presented below.

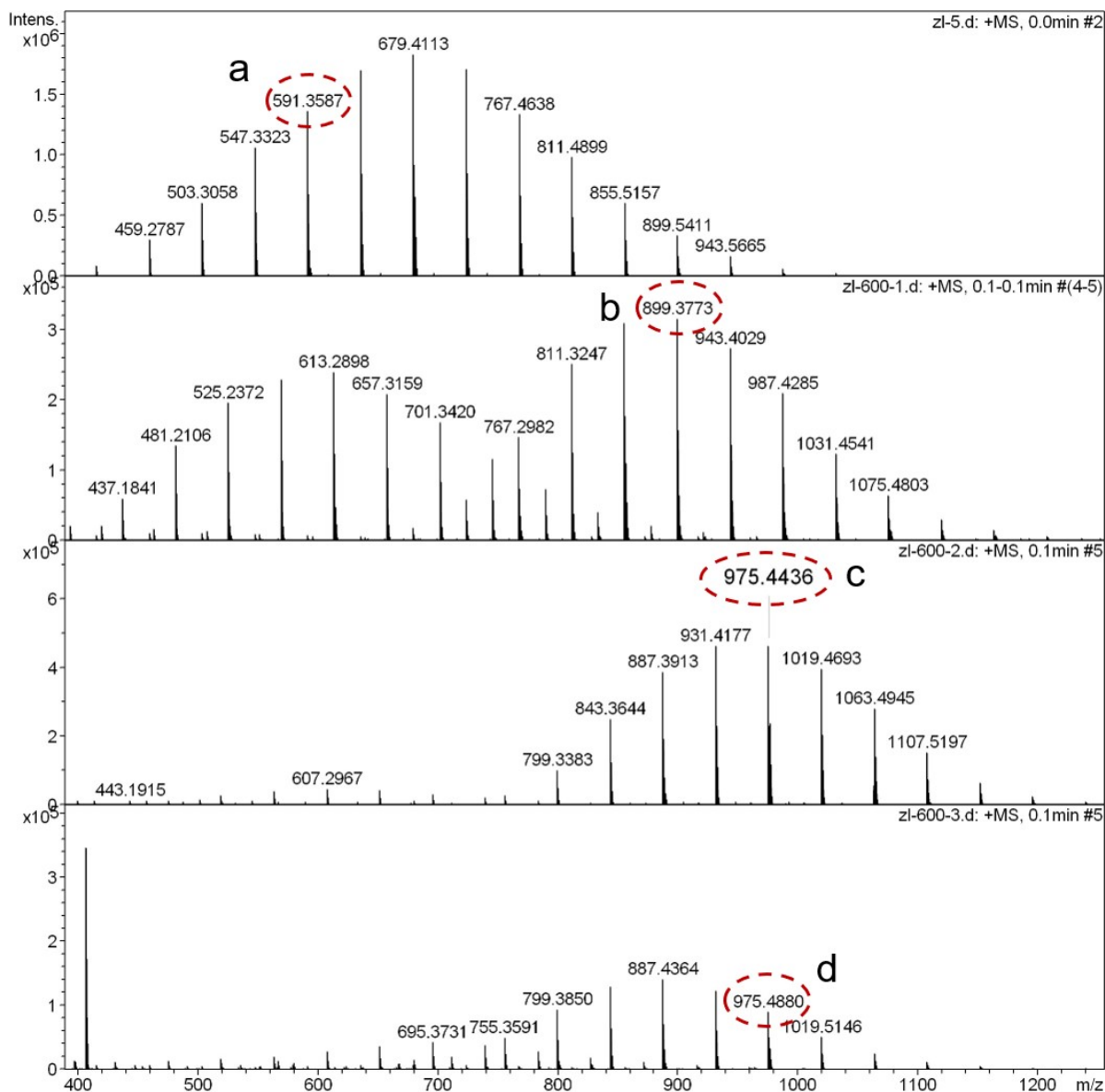


Figure S25. HR-MS spectra of the compound PEG-600 (a), TsO-PEG-600-Ots (b), DTH-dimer-600-ester (c), and DTH-dimer-600 (d).